Magnesium ferrite nanostructures for detection of ethanol vapours - A first-principles study

Veerappan Nagarajan, Arunachalam Thayumanavan, Ramanathan Chandiramouli*

School of Electrical & Electronics Engineering, SASTRA University, Tirumalaisamudram, Thanjavur - 613 401, India

Abstract

The adsorption behaviour and electronic properties of ethanol vapour on $MgFe_2O_4$ ceramic nanostructures are studied using density functional theory technique. The structural stability of $MgFe_2O_4$ nanostructure is determined with the help of formation energy. The adsorption behaviour of ethanol molecules on $MgFe_2O_4$ base material is analysed in terms of average energy gap variation, Mulliken charge transfer, band gap and adsorption energy. The most prominent adsorption sites of ethanol vapours on $MgFe_2O_4$ nanostructure are investigated at atomistic level. The density of states spectrum reveals the clear picture about the electronic properties of $MgFe_2O_4$ nanostructure. The density of states and electronic band gap confirmed the adsorption of ethanol vapours on $MgFe_2O_4$ nanostructure. The changes in the energy band gap and density of states are observed upon adsorption of ethanol vapour molecules on $MgFe_2O_4$ nanostructure. The density of states spectrum also confirms the changes in peak maxima due to the transfer of electrons between $MgFe_2O_4$ nanostructure and ethanol vapours. The adsorption of oxygen atom from ethanol vapour on iron in $MgFe_2O_4$ is found to be more prominent rather than other adsorption sites. The findings show that $MgFe_2O_4$ nanostructure can be utilized to sense the presence of ethanol vapour in the atmosphere.

Keywords: $MgFe_2O_4$, adsorption, , formation energy, ethanol, energy gap

I. Introduction

The solid state gas/vapour sensor is in demand to monitor the atmospheric pollutants and the environment. Moreover, rapid response of chemical sensor is required to improve the quality and performance of gas/vapour sensors. Alcohol vapour sensors can be utilized for monitoring fermentation process [1], breath analyser and food packaging test [2]. In general, the environment contains small amount of alcohol vapour molecules such as ethanol and methanol, which are highly toxic molecules. Especially, these vapours are hazardous to the human central nervous system, resulting in coma, blindness and death. Furthermore, inhalation of high concentration of alcohol vapour molecules can damage brain and other organs permanently. Thus, there is a need to develop a high performance gas/vapour sensor for alcohol detection.

Magnesium ferrite ($MgFe_2O_4$) is one of the promi-

nent spinel structured n-type semiconductor materials with direct band gap of 1.9 eV [3], which can be effectively used in various fields, including hyperthermia [4], sensor [5], metal ion removal [6], anode materials [7], azo-dye degradation [8] and photocatalysts [9]. In addition, $MgFe_2O_4$ exhibits high resistivity, low dielectric and magnetic losses, hence it is a significant system in heterogeneous catalysis, sensors and adsorption [10]. For any gas/vapour sensor, its sensing properties are highly related to the microstructural characteristics of the system, which directly depend on its synthesis method [11]. Doroftei *et al.* [12] reported that $MgFe_2O_4$ material shows a good response towards ethanol molecules at 380 °C using auto-combustion method. Kaur *et al.* [13] reported the surface areas of magnesium ferrite when prepared by co-precipitation, solution combustion and sol-gel method with the help of urea, oxalyl dihydrazide and polyethylene glycol as fuels, respectively. Evidently, various compositions of spinel ferrite structures as well as their synthesizing methods alter their vapour sensing properties [14,15].

* Corresponding author: tel: +91 9489 566466
fax.:+91 4362 264120, e-mail: *rcmoulii@gmail.com*

Godbole *et al.* [16] reported about $MgFe_2O_4$ nanoparticles as a rapid gas sensor towards alcohol vapour molecules. Liu *et al.* [17] synthesized the magnesium ferrite nanoparticles and investigated their gas sensing properties towards H_2S, CH_4, ethanol and LPG vapours. Jeseentharani *et al.* [18] synthesized various metal ferrites including $MgFe_2O_4$ material and studied their humidity sensing properties. In our previous work [19], we demonstrated the adsorption of H_2S gas on α-Fe_2O_3 nanostructures. Therefore, tailoring the electronic properties of $MgFe_2O_4$ ceramics inspired the present study to investigate the adsorption behaviour of ethanol vapour molecules on magnesium ferrite. The adsorption of oxygen and hydrogen atom from the ethanol molecule on spinel structured $MgFe_2O_4$ nanostructure is investigated and the obtained results are reported.

II. Computational details

The spinel $MgFe_2O_4$ structure with space group of $Fd\bar{3}m$ (227) was used in the present study. The $MgFe_2O_4$ nanostructure is investigated with the help of density functional theory using SIESTA package [20]. The local geometry relaxation was performed with generalized gradient approximation (GGA) in combination with exchange-correlation functional Perdew-Burke-Ernzerhof (PBE) level of theory including van der Waals (vdW) dispersion correction implemented by vdW-DF [21]. Presently, the vdW-DF function is implemented in SIESTA code [21], which has been utilized for computing metal organic materials [22,23]. Furthermore, this vdW-DF function somehow reduces the underestimation of the energy band gap. The Perdew-Burke-Ernzerhof function is more suitable for studying spinel ferrites, which is validated by previous reports in literature [24]. For structural optimization of $MgFe_2O_4$, the energy cutoff is adjusted to 400 eV and the geometry relaxation was performed until the force and energy were converged to 0.02 eV/Å and 10^{-6} eV, respectively. The Brillouin zones of $MgFe_2O_4$ nanostructure are sampled with $5 \times 5 \times 5$ k-point of the Monkhorst-pack. The electronic band structures, density of states, charge density and electron localization function (ELF) of $MgFe_2O_4$ nanostructure were computed using SIESTA code. The approximation of transfer of electron is based on Mulliken charge analysis [25]. The ethanol adsorption properties on $MgFe_2O_4$ nanostructure were also investigated using SIESTA package. In the present study, the double zeta polarization (DZP) basis set is utilized for optimizing $MgFe_2O_4$ nanostructures [26,27].

III. Results and discussion

3.1. Structure of MgFe2O4

The present study is focused to investigate the structural stability of cubic $MgFe_2O_4$ spinel nanostructure and to use $MgFe_2O_4$ nanostructure to investigate the adsorption behaviour of ethanol in terms of electronic

band gap, Mulliken charge transfer and adsorption energy. Figure 1 refers to the schematic diagram of $MgFe_2O_4$ nanostructure with applied periodic boundary condition (PBC). The periodic boundary conditions on proposed cubic $MgFe_2O_4$ spinel structure are used to reduce the edge effects. Furthermore, the $MgFe_2O_4$ nanostructures are approximate and equivalent in an infinite array. Thus, we have chosen $MgFe_2O_4$ spinel type nanostructure with applied PBC along the cubic face, which are utilized in the computation work.
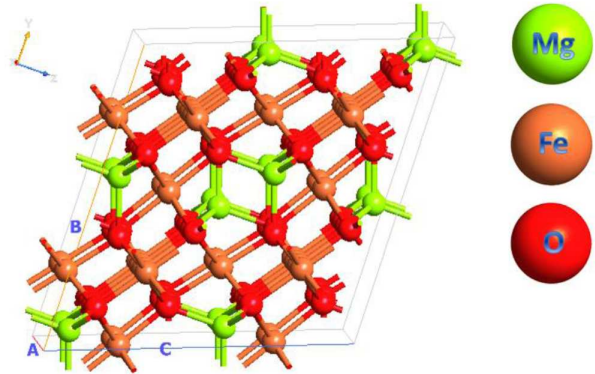

Figure 1. Schematic diagram of MgFe₂O₄ nanostructure

The structural formula of $MgFe_2O_4$ is generally expressed as $(Mg_{1-x}^{2+}Fe_x^{3+})[Mg_x^{2+}Fe_{2-x}^{3+}]O_4$, where square and round brackets refer to cation sites of octahedral [B] and tetrahedral (A) coordinates, respectively, and x represents the degree of inversion (which is ascertained as the fraction of A-sites filled by Fe^{3+} cations). The tunable chemical and physical properties of spinel ferrites arose from their ability to transfer the cations among the octahedral [B] and tetrahedral (A) sites [28]. In the present work, the base material consists of $MgFe_2O_4$ nanostructure, which has sixteen Mg atoms, thirty two Fe atoms and sixty four O atoms in order to confirm the stoichiometry in the structure. The adsorption behaviour and electronic properties of ethanol molecule on $MgFe_2O_4$ nanostructure are investigated and the results are discussed.

In general, the structural stability of $MgFe_2O_4$ nanostructure can be determined using formation energy [29,30] as expressed in equation (1):

$$E_{form} = 1/n[E(MFO-n) - xE(Mg) - yE(Fe) - zE(O)] \quad (1)$$

where $E(MFO-n)$ refers to the total energy of $MgFe_2O_4$ nanostructure, E(Mg), $E(Fe)$ and $E(O)$ are the corresponding energy of isolated Mg, Fe and O atoms and n is the total number of atoms in $MgFe_2O_4$ nanostructure. Besides, x, y and z refer to the number of Mg, Fe and O atoms, respectively. In this work, the formation energy of $MgFe_2O_4$ nanostructure is found to be -5.89 eV, which infers the stability of $MgFe_2O_4$ nanostructure.
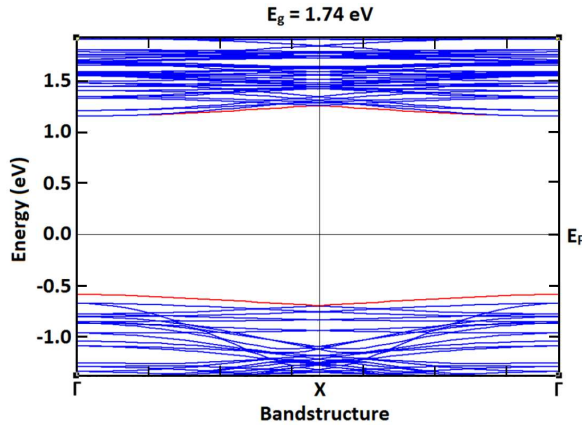
Figure 2. Energy band structure of isolated MgFe₂O₄ nanostructure

3.2. Electronic properties of MgFe₂O₄ nanostructure

The inspiration behind the present study is to investigate the adsorption behaviour and electronic properties of ethanol on $MgFe_2O_4$ nanostructure. The electronic properties of $MgFe_2O_4$ nanostructure material are described in terms of energy band structure. Figure 2 shows the electronic band gap of isolated $MgFe_2O_4$ nanostructure. The band gap of $MgFe_2O_4$ ceramics is observed to be 1.74 eV near the gamma point (Γ). Furthermore, the observed band gap of $MgFe_2O_4$ nanostructure is validated with the reported experimental work (1.90 eV [3]). Benko *et al.* [31] reported the effect of defects on photoelectrochemical properties of $MgFe_2O_4$ semiconductor and estimated the experimental band gap of 2.18 eV. The band gap of $MgFe_2O_4$ nanostructure may be underestimated in the present study; since the density functional calculation with GGA/PBE exchange-correlation functional is used to study electron-electron interaction in their respective ground state. Moreover, the electronic and adsorption behaviour of ethanol in $MgFe_2O_4$ base material remains unchanged even though the band gap is underestimated.

The density of states (DOS) spectrum [32,33] gives the perception of localization of charges in different energy intervals along $MgFe_2O_4$ nanostructure. Figure 3 represents the projected density of states (PDOS) and DOS spectrum of the isolated $MgFe_2O_4$ nanostructure. The peak maxima are noticed closer to the Fermi energy level (E_F) for isolated $MgFe_2O_4$ nanostructure, which is favourable for the adsorption of target vapour/gas molecules that illustrates the transfer of electrons between $MgFe_2O_4$ nanostructure and ethanol vapour molecules. The peak maximum in different energy intervals is observed owing to the overlapping of molecular orbitals among Mg, Fe and O atoms in $MgFe_2O_4$ material.

In general, with chemi-resistive type of sensor, the current flowing through the molecular device is directly related to the amount of gas/vapour present in the atmosphere. From the observation of electronic band structure and DOS spectrum of $MgFe_2O_4$ nanostructure, it is confirmed that $MgFe_2O_4$ material can be utilized as chemi-resistive sensor.

3.3. Adsorption of ethanol vapour on MgFe₂O₄

In the beginning stage of adsorption study of ethanol molecules on $MgFe_2O_4$ base material, bond lengths of the system must be relaxed. The optimized bond lengths between the Mg & O and Fe & O are found to be 2.001 Å and 2.059 Å, respectively. In addition, we have also carried out the vibrational frequency calculation to verify that all relaxed spinel nanostructures are related to global minima. Moreover, in the present work we mainly focused on five different adsorption sites with global minima position as follows:

$$C_2H_5OH + 3O_{2(ads)}^- \xrightarrow{MgFe_2O_4 surface} 2\,CO_2\uparrow + 3\,H_2O\uparrow + 3\,e^- \quad (2)$$
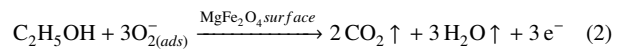
Figures 4a,b represent H and O atoms from ethanol vapour molecules interacting with an Mg atom in $MgFe_2O_4$ nanostructure named as positions A and B, respectively. Figures 4c,d illustrate H and O atoms from ethanol adsorbed on Fe atom in $MgFe_2O_4$ nanostructure mentioned as position C and position D, respectively. Figure 4e represents the interaction of H atom from
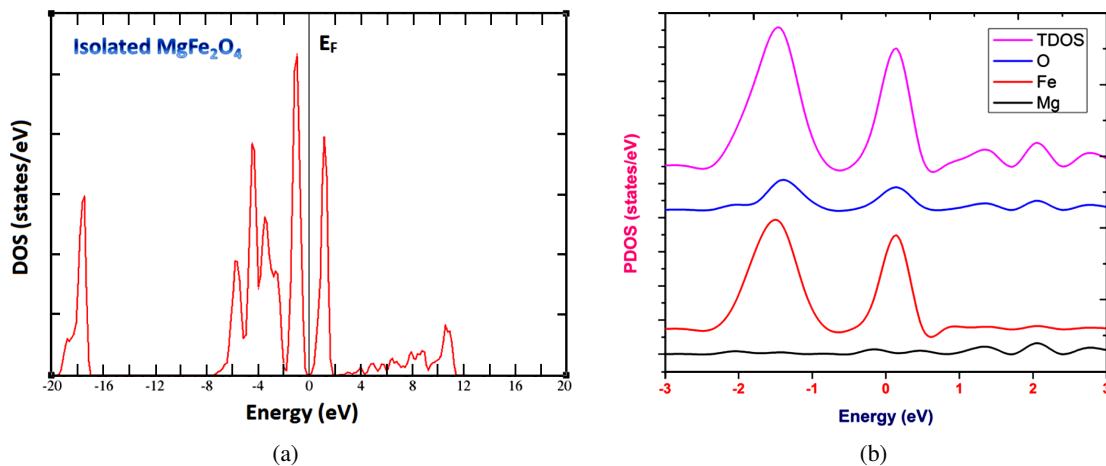

(a)

(b)

Figure 3. Projected density of states (PDOS) and density of states (DOS) spectrum of the isolated MgFe₂O₄ nanostructure
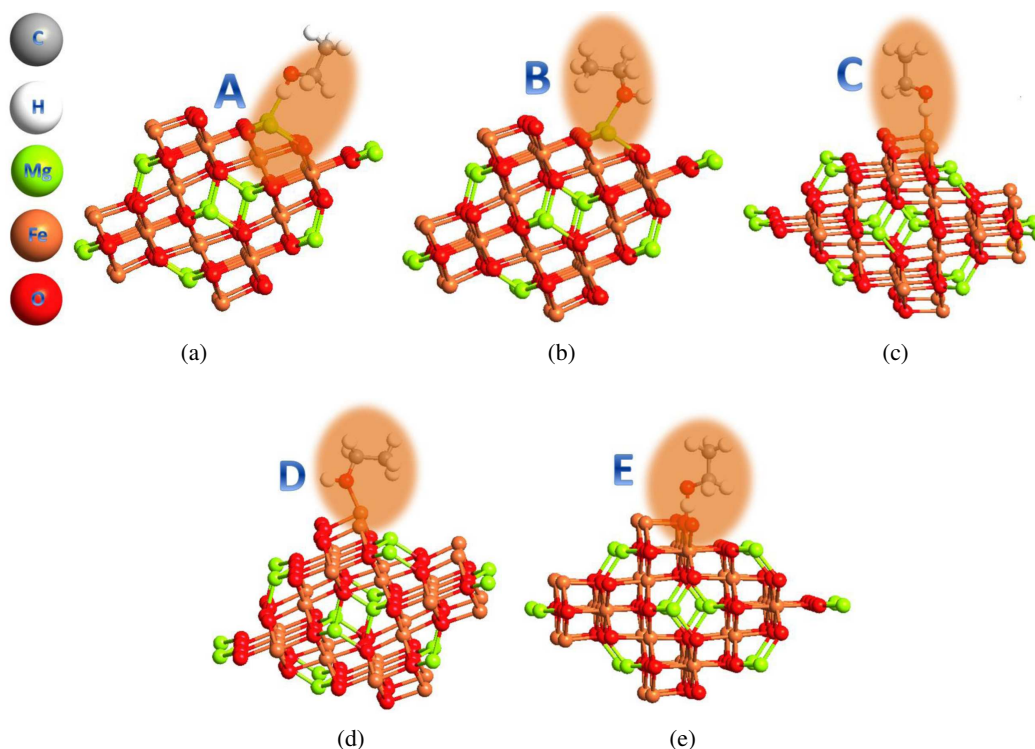
Figure 4. Ethanol interaction on position: a) A, b) B, c) C, d) D and e) E

ethanol molecules with O atom in $MgFe_2O_4$ nanostructure, which is mentioned as position E.

The sensing mechanism and adsorption energy of ethanol vapour molecules on $MgFe_2O_4$ nanostructure can be expressed using the equations (2) and (3) as:

$$E_{ad} = E(MFO/Et) - E(MFO) - E(Et) + E(BSSE) \quad (3)$$

where $E(MFO/Et)$ refers the energy of $MgFe_2O_4/CH_3CH_2OH$. The isolated energy of $MgFe_2O_4$ nanostructure is represented as $E(MFO)$ and $E(Et)$ infers the isolated energy of ethanol molecules. In order to eliminate the overlap effects on different basis functions, basis set superposition error (BSSE) [34] has been used in terms of counterpoise method. When volatile organic compounds (VOCs) get adsorbed on $MgFe_2O_4$ nanostructure, the negative value of the adsorption energy (E_{ad}) infers the adsorption of ethanol vapour molecules on $MgFe_2O_4$ nanostructure. In this work, almost all the adsorption sites from A to E show the negative value of adsorption energy. It implies that the ethanol molecule gets adsorbed on $MgFe_2O_4$ nanostructure. The adsorption energy of $MgFe_2O_4$ nanostructure for the positions A to E is observed to be -1.75, -2.60, -3.96, -2.08 and $-1.87\,eV$, respectively. Moreover, the electronic band gap of $MgFe_2O_4$ nanostructure varies owing to the adsorption of ethanol molecules on various prominent sites of the base material. During the adsorption process, transfer of electrons takes place between $MgFe_2O_4$ material and ethanol molecules resulting in the variation of resistance in $MgFe_2O_4$ nanostructure. Moreover, the

variation in the resistance of $MgFe_2O_4$ can be measured using simple 2-probe technique in which the changes in the resistance are directly related to the amount of ethanol vapour molecules [35]. The narrowing of the band gap of $MgFe_2O_4$ nanostructure upon adsorption of ethanol molecule is governed by the rapid transfer of electrons between the $MgFe_2O_4$ material and ethanol vapour, which in turn enhances the conductivity of $MgFe_2O_4$ nanostructure. Figure 5 shows the energy band gap of $MgFe_2O_4$ nanostructure for positions A, B, C, D and E, respectively.

The changes in the band gap of $MgFe_2O_4$ nanostructure for the positions from A to E are noticed to be 0.53, 0.41, 0.64, 0.20 and 0.44 eV, respectively. Therefore, the changes in the energy band gap upon adsorption of ethanol molecules on $MgFe_2O_4$ nanostructure and adsorption energy clearly show that $MgFe_2O_4$ nanostructure can be efficiently used for the detection of ethanol vapour. Benko *et al.* [31] reported that magnesium ferrite has the energy band gap value of 2.18 eV. Recently, Fan *et al.* [3] have also confirmed that the energy band gap of pristine $MgFe_2O_4$ material as 1.9 eV, which supports the present work. The validation of the present study with previously reported work is a significant criterion. Zhang *et al.* [36] proposed the inverse spinel structure $MgFe_2O_4$ with Pt catalyst ($Pt/MgFe_2O_4$), which provides efficient catalytic properties for CO oxidation below the normal humidity and temperature. Jeseentharani *et al.* [18] synthesized the various metal ferrites including $CoFe_2O_4$, $MgFe_2O_4$, using solid-state reaction. These ferrites nanoparticles have been efficiently used as humidity sensors. Liu *et*
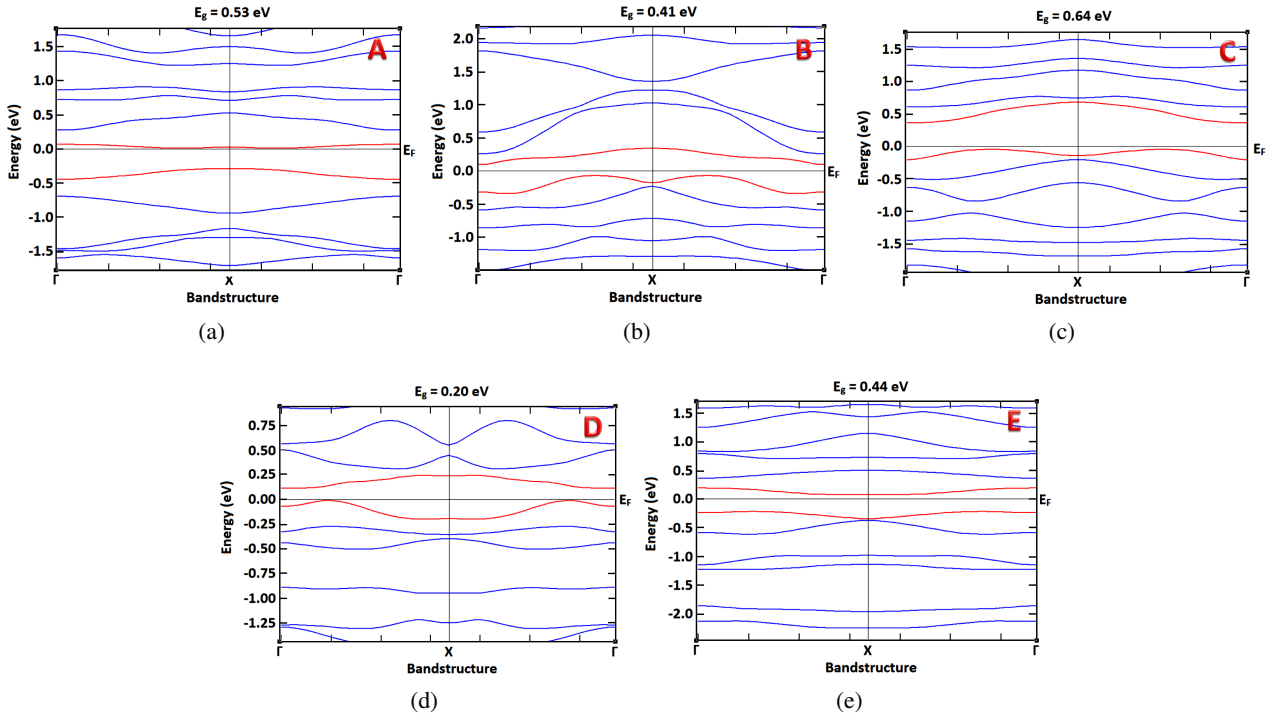
Figure 5. Energy band structure of position: a) A, b) B, c) C, d) D and e) E

al. [17] synthesized $MgFe_2O_4$ using solid-state reaction and demonstrated gas/vapour sensing towards H_2S, CH_4, ethanol and LPG. Recently, Godbole *et al.* [16] experimentally confirmed that $MgFe_2O_4$ can be utilized for the alcohol vapour sensor. From the literature, we noticed that there are no computational works reported on $MgFe_2O_4$ nanostructure as an ethanol sensor using first-principles studies. Moreover, the most favourable adsorption site of ethanol vapour molecule on $MgFe_2O_4$ base material can be found only after investigating the percentage of average energy gap variation compared to its isolated counterpart. Table 1 represents the energy band gap, Mulliken charge transfer, percentage of average energy band gap variation and adsorption energy. As a result, it is clearly revealed that $MgFe_2O_4$ nanostructure is a good candidate for ethanol vapour detection. Accordingly, $MgFe_2O_4$ nanostructure exhibits good sensing response at all prominent adsorption sites. However, it is noticed that the interaction of O atom from an ethanol molecule with Fe atom in $MgFe_2O_4$ material is more prominent than other adsorption sites, which is precisely verified by average energy gap variation.

The other significant deciding factor to investigate the adsorption of ethanol vapour on $MgFe_2O_4$ material is described in terms of transfer of electrons, which is examined by Mulliken charge transfer (Q) [37–39]. The positive value of Mulliken charge infers the transfer of free electrons from ethanol vapours to $MgFe_2O_4$ nanostructure. In contrast, the negative magnitude of the Mulliken charge transfer confirms that the unbound electrons are transferred from $MgFe_2O_4$ material to the ethanol vapour molecules [40–42]. The Mulliken charge transfer for various positions A to E are found to be $0.678\,e$, $0.699\,e$, $1.630\,e$, $0.893\,e$ and $0.170\,e$, respectively. It is evident that positive value of Mulliken charge is observed when ethanol molecules get adsorbed on $MgFe_2O_4$ nanostructure. The large variation of the energy band gap is observed for position D with a moderate positive value of Mulliken charge together with a corresponding minimum value of adsorption energy. However, for position C high positive magnitude of Mulliken charge with low value of energy band gap variation is noticed, even though the corresponding adsorption energy values are found to be high. Interestingly, for position A and B almost the same values of

Table 1. Mulliken charge, adsorption energy and average energy gap variation of $MgFe_2O_4$ nanostructure

Nanostructure	E_{ad} [eV]	Q [e]	E_g [eV]	E_g^a [%]
Isolated $MgFe_2O_4$	-	-	1.74	-
Position A	−1.75	0.678	0.53	228.30
Position B	−2.60	0.699	0.41	324.39
Position C	−3.96	1.630	0.64	171.88
Position D	−2.08	0.893	0.2	770.00
Position E	−1.87	0.170	0.44	295.46

Mulliken charge with different negative values of adsorption energy are observed along with the changes in average energy gap variation. Thus, we conclude that the adsorption of O atom from ethanol molecules interacting with Fe atom in $MgFe_2O_4$ nanostructure is observed to be the most favourable adsorption event.

Figure 6 illustrates the electron density of isolated $MgFe_2O_4$ nanostructure upon adsorption of ethanol molecules. From the electron density diagram it is confirmed that the electron density is higher along the hydroxyl group (adsorption site) upon adsorption on $MgFe_2O_4$ material. Thus, the transfer of electrons is noticed during the adsorption of ethanol vapour molecules, which strengthens presumption that $MgFe_2O_4$ nanostructure act as a chemi-resistor material for the sensing of ethanol vapour molecules.

Figure 7 shows the projected density of states (PDOS) and density of states (DOS) spectrum of $MgFe_2O_4$ nanostructure for the positions A to E. From this, it is evident that the more peak maxima are observed in LUMO level of $MgFe_2O_4$ nanostructure. This implies that the free electrons can easily transfer between $MgFe_2O_4$ nanostructure and ethanol molecules, which confirms the use of $MgFe_2O_4$ material as chemical sensor.

IV. Conclusions

Electronic properties and adsorption behaviour of ethanol molecules on $MgFe_2O_4$ nanostructure are studied using the DFT technique with GGA/PBE exchange-correlation functional. The density of states spectrum reveals the peak maxima closer to the Fermi energy level and the band gap of $MgFe_2O_4$ nanostructure is observed to be 1.74 eV. However, the adsorption of ethanol molecules on $MgFe_2O_4$ is confirmed with the changes on Mulliken charge transfer, energy band gap and adsorption energy. The results from the DOS spectrum and energy band gap variation clearly show that the electron transfer takes place between $MgFe_2O_4$ nanostruc-
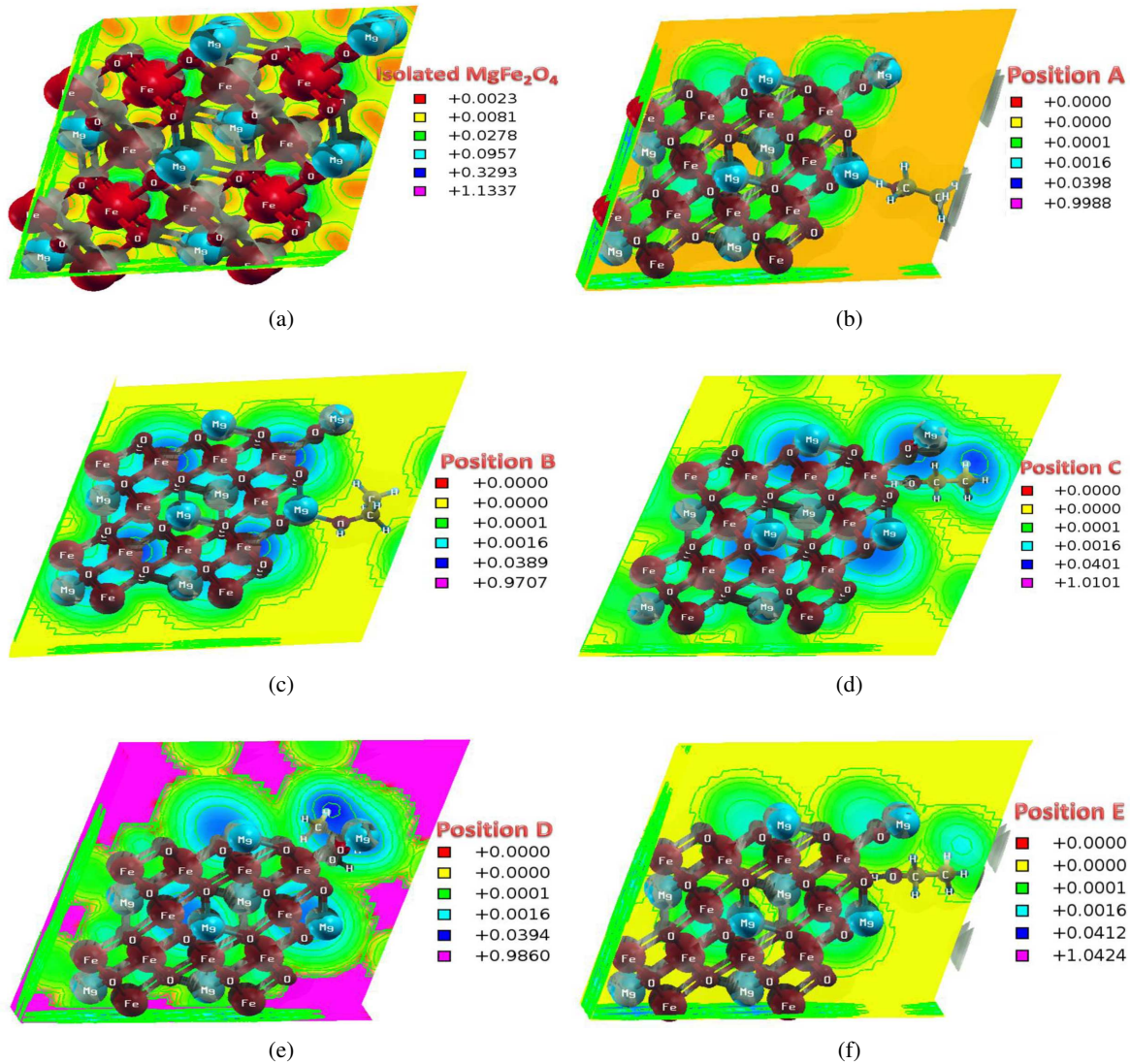

Figure 6. Electron density of: a) isolated $MgFe_2O_4$ nanostructure, b) position A, c) position B, d) position C, e) position D and f) position E
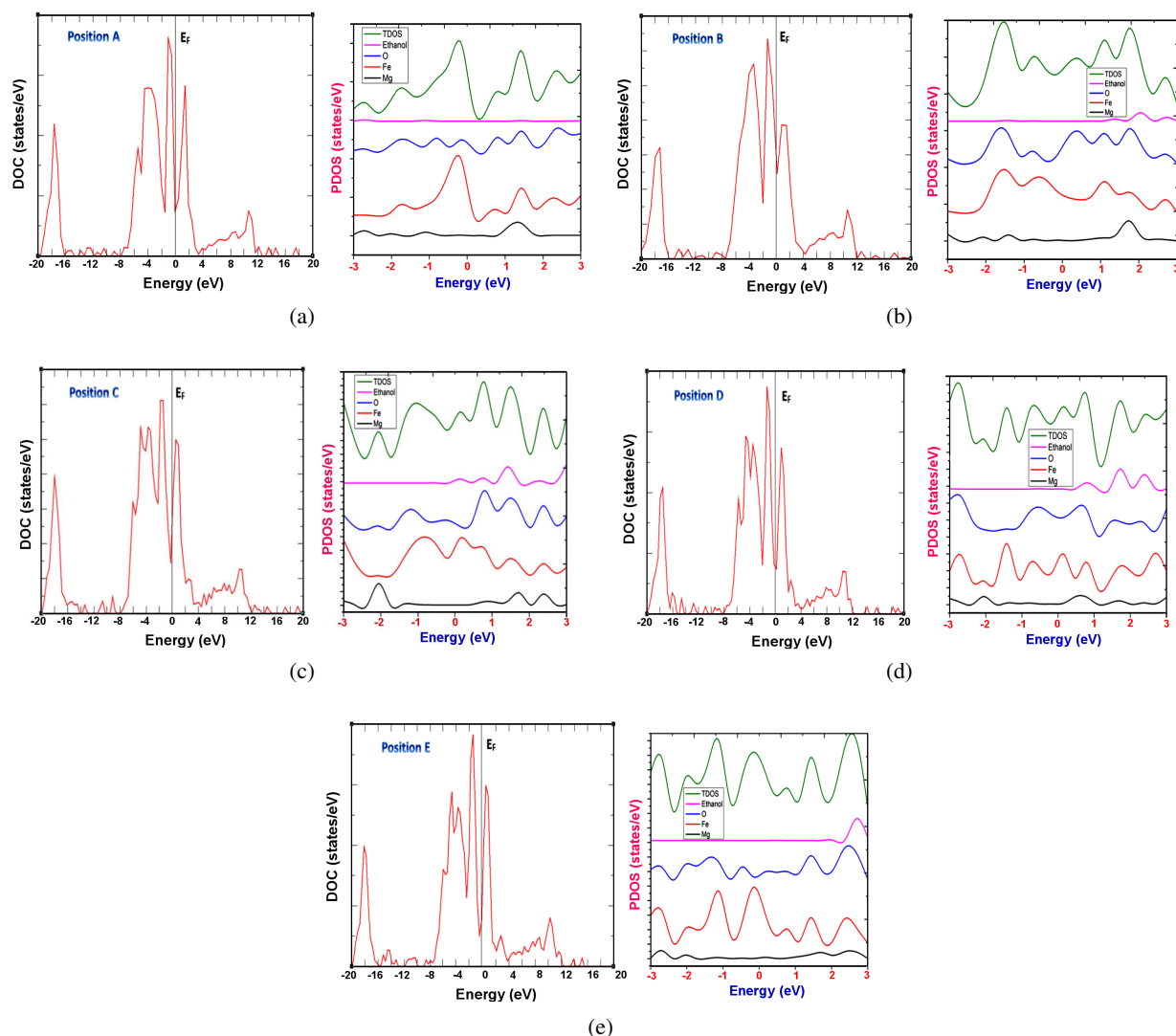
Figure 7. Projected density of states (PDOS) and density of states (DOS) spectrum of position: a) A, b) B, c) C, d) D and e) E

ture and ethanol molecules, which is verified with the variation in the peak maxima along the conduction band and the valence band. Moreover, the prominent adsorption site is studied at atomistic level. It is shown that the most favourable adsorption mechanism is interaction of O atom from ethanol molecules with Fe atom in $MgFe_2O_4$ nanostructure. From the overall results, it can be concluded that the $MgFe_2O_4$ ceramic material can be effectively utilized to sense the presence of ethanol vapour molecules in the atmosphere.

References

1. B.P.J.D.L. Costello, R.J. Ewen, H.E. Gunson, N.M. Ratcliffe, P.T.N. Spencer-Phillips, "The development of a sensor system for the early detection of soft rot in stored potato tubers", *Meas. Sci. Technol.*, **11** (2000) 1685–1691.
2. J.J. Ho, Y.K. Fang, K.H. Wu, W.T. Hsieh, C.H. Chen, M.S. Ju, J.J. Lin, S.B. Hwang, "High sensitivity ethanol vapor sensor integrated with a solid-state heater and a thermal isolation improvement for legal drink-drive limit detecting", *Sensor. Actuat. B*, 50 (1998) 227–233.
3. W.Q. Fan, M. Li, H.Y. Bai, D.B. Xu, C. Chen, C.F. Li, Y.L. Ge,W.D. Shi, "Fabrication of $MgFe_2O_4$/MoS_2 heterostructure nanowires for photoelectrochemical catalysis", *Langmuir*, **32** (2016) 1629–1636.
4. M. Bagheri, M.A. Bahrevar, A. Beitollahi, "Synthesis of mesoporous magnesium ferrite ($MgFe_2O_4$) using porous silica templates", *Ceram. Int.*, **41** (2015) 11618–11624.
5. R.V. Godbole, P. Rao, P.S. Alegaonkar, S. Bhagwat, "Influence of fuel to oxidizer ratio on LPG sensing performance of $MgFe_2O_4$ nanoparticles", *Mater. Chem. Phys.*, **161** (2015) 135–141.
6. V. Srivastava, Y.C. Sharma, M. Sillanpää, "Application of nano-magnesso ferrite (n-$MgFe_2O_4$) for the removal of Co^{2+} ions from synthetic wastewater: Kinetic, equilibrium and thermodynamic studies", *Appl. Surf. Sci.*, **338** (2015) 42–54.
7. Y.H. Yin, N.N. Huo, W.F. Liu, Z.P. Shi, Q.X. Wang, Y.M. Ding, J. Zhang, S.T. Yang, "Hollow spheres of $MgFe_2O_4$ as anode material for lithium-ion batteries", *Scripta Mater.*, **110** (2016) 92–95.
8. J. Gao, S.G. Yang, N. Li, L.J. Meng, F. Wang, H. He, C. Sun, "Rapid degradation of azo dye Direct Black BN by magnetic $MgFe_2O_4$-SiC under microwave radiation",

Appl. Surf. Sci., **379** (2016) 140–149.

9. K. Tezuka, M. Kogure, Y.J. Shan, "Photocatalytic degradation of acetic acid on spinel ferrites MFe$_2$O$_4$ (M = Mg, Zn, and Cd)", *Catal. Commun.*, **48** (2014) 11–14.

10. M. Tada, T. Kanemaru, T. Hara, T. Nakagawa, H. Handa, M. Abe, "Synthesis of hollow ferrite nanospheres for biomedical applications", *J. Magn. Magn. Mater.*, **321** (2009) 1414–1416.

11. S. Bangale, V. Chaugule, R. Prakshale, S. Bamane, "Microbial gas-sensing property of Escherichia coli with mixed metal catalyst MgFe$_2$O$_4$", *Curr. Sci.*, **105** (2013) 984–989.

12. C. Doroftei, E. Rezlescu, N. Rezlescu, P.D. Popa, "Magnesium ferrite with Sn^{4+} and/or Mo^{6+} substitutions as sensing element for acetone and ethanol", *Rom. J. Phys.*, **51** (2006) 631–640.

13. N. Kaur, M. Kaur, "Comparative studies on impact of synthesis methods on structural and magnetic properties of magnesium ferrite nanoparticles", *Process. Appl. Ceram.*, **8** (2014) 137–143.

14. N. Iftimie, E. Rezleseu, P.D. Popa, N. Rezlescu, "On the possibility of the use of a nickel ferrite as semiconducting gas sensor", *J. Optoelectron. Adv. Mater.*, **7** (2005) 911–914.

15. W. Jander, "Reaction between basic and acid oxides and carbonates and method of compound formation", *Z. Anorg. Allg. Chem.*, **174** (1928) 11–23.

16. R. Godbole, P. Rao, S. Bhagwat, "Magnesium ferrite nanoparticles: a rapid gas sensor for alcohol", *Mater. Res. Express*, **4** (2017) 025032.

17. Y.-L. Liu, Z.-M. Liu, Y. Yang, H.-F. Yang, G.-L. Shen, R.-Q. Yu, "Simple synthesis of MgFe$_2$O$_4$ nanoparticles as gas sensing materials", *Sensor. Actuat. B*, **107** (2005) 600–604.

18. V. Jeseentharani, M. George, B. Jeyaraj, A. Dayalan, K.S. Nagaraja, "Synthesis of metal ferrite (MFe$_2$O$_4$, M = Co, Cu, Mg, Ni, Zn) nanoparticles as humidity sensor materials", *J. Exp. Nanosci.*, **8** (2013) 358–370.

19. V. Nagarajan, R. Chandiramouli, "DFT studies on interaction of H$_2$S Ggas with α-Fe$_2$O$_3$ nanostructures", *J. Inorg. Organomet. Polym.*, **26** (2016) 394–404.

20. J.M. Soler, E. Artacho, J.D. Gale, A. Garcia, J. Junquera, P. Ordejon, D. S-Portal, "The SIESTA method for ab initio order-N materials simulation", *J. Phys.: Condens. Mat.*, **14** (2002) 2745–2779.

21. G. Roman-Perez, J.M. Soler, "Efficient implementation of a van der Waals density functional: Application to double-wall carbon nanotubes", *Phys. Rev. Lett.*, **103** (2009) 096102.

22. A.M. Walker, B. Civalleri, B. Slater, C. Mellot-Draznieks, F. Corà, C.M. Zicovich-Wilson, G. Román-Pérez, J.M. Soler, J.D. Gale, "Flexibility in a metal-organic framework material controlled by weak dispersion forces: The bistability of MIL-53(Al)", *Angew. Chemie - Int. Ed.*, **49** (2010) 7501–7503.

23. L. Kong, G. Roman-Perez, J.M. Soler, D.C. Langreth, "Energetics and dynamics of H$_2$ adsorbed in a nanoporous material at low temperature", *Phys. Rev. Lett.*, **103** (2009) 096103.

24. J. Yao, Y. Li, X. Li, X. Zhu, "First-principles study of the geometric and electronic structures of zinc ferrite with vacancy defect", *Metall. Mater. Trans. A*, **47A** (2016) 3753–3760.

25. V. Nagarajan, R. Chandiramouli, "Interaction of NH$_3$ gas on α-MoO$_3$ nanostructures - A DFT investigation", *Condens. Mat. Phys.*, **20** [2] (2017) 23705.

26. T.H. Dunning, "Gaussian basis functions for use in molecular calculations. I. Contraction of (9s5p)(9s5p) atomic basis sets for the first-row atoms", *J. Chem. Phys.*, **53** (1970) 2823.

27. P.C. Hariharan, J.A. Pople, "The influence of polarization functions on molecular orbital hydrogenation energies", *Theor. Chim. Acta*, **28** (1973) 213–222.

28. M. Soliman Selim, G. Turky, M.A. Shouman, G.A. El-Shobaky, "Effect of Li$_2$O doping on electrical properties of CoFe$_2$O$_4$", *Solid State Ionics*, **120** (1999) 173–181.

29. R. Chandiramouli, V. Nagarajan, "Borospherene nanostructure as CO and NO sensor - A first-principles study", *Vacuum*, **142** (2017) 13–20.

30. V. Nagarajan, R. Chandiramouli, "Adsorption studies of ethanol and butanol on Co$_3$O$_4$ nanostructures - A DFT study", *Chem. Phys.*, **491** (2017) 61–68.

31. F.A. Benko, F.P. Koffyberg, "The effect of defects on some photoelectrochemical properties of semiconducting MgFe$_2$O$_4$", *Mater. Res. Bull.*, **21** (1986) 1183–1188.

32. S. Harsha Varthan, V. Nagarajan, R. Chandiramouli, "First-principles insights on mechanical and electronic properties of TiX (X = C, N) in β-Si$_3$N$_4$ based ceramics", *Process. Appl. Ceram.*, **10** [3] (2016) 153–160.

33. M. Eslami, V. Vahabi, A.A. Peyghan, "Sensing properties of BN nanotube toward carcinogenic 4-chloroaniline: A computational study", *Physica E*, **76** (2016) 6–11.

34. M. Noei, A.-A.Salari, M. Madani, M. Paeinshahri, H. Anaraki-Ardakani, "Adsorption properties of CH$_3$COOH on (6,0), (7,0), and (8,0) zigzag, and (4,4), and (5,5) armchair single-walled carbon nanotubes: A density functional study", *Arab. J. Chem.*, **10** (2017) S3001–S3006.

35. R. Chandiramouli, B.G. Jeyaprakash, "Operating temperature dependent ethanol and formaldehyde detection of spray deposited mixed CdO and MnO$_2$ thin films", *RSC Adv.*, **5** (2015) 43930–43940.

36. B. Zheng, S. Wu, X. Yang, M. Jia, W. Zhang, G. Liu, "Room temperature CO oxidation over Pt/MgFe$_2$O$_4$: A stable inverse spinel oxide support for preparing highly efficient Pt catalyst", *ACS Appl. Mater. Interf.*, **8** (2016) 26683–26689.

37. R.S. Mulliken, "Electronic population analysis on LCAOMO molecular wave functions", *J. Chem. Phys.*, **23** (1955) 1833–1840.

38. V. Nagarajan, R. Chandiramouli, "Interaction of alcohols on monolayer stanane nanosheet: A first-principles investigation", *Appl. Surf. Sci.*, **419** (2017) 9–15.

39. M.T. Baei, A.A. Peyghan, Z. Bagheri, "Ab initio study of NH$_3$ and H$_2$O adsorption on pristine and Na-doped MgO nanotubes", *Struct. Chem.*, **24** (2013) 165–170.

40. V. Nagarajan, R. Chandiramouli, "Borophene nanosheet molecular device for detection of ethanol - A first-principles study", *Comput. Theor. Chem.*, **1105** (2017) 52–60.

41. T.P. Kaloni, "Tuning the structural, electronic, and magnetic properties of germanene by the adsorption of 3d transition metal atoms", *J. Phys. Chem. C*, **118** [43] (2014) 25200–25208.

42. J. Beheshtian, I. Ravaei, "Toxic CO detection by Li-encapsulated fullerene-like BeO", *Struct Chem.*, (2017) DOI: 10.1007/s11224-017-1022-z.